

## Superconducting phase of $\text{La}_2\text{CuO}_{4+\delta}$ : A superconducting composition resulting from phase separation

J. D. Jorgensen, B. Dabrowski, Shiyou Pei, D. G. Hinks, and L. Soderholm

*Materials Science and Chemistry Divisions, Argonne National Laboratory, Argonne, Illinois 60439*

B. Morosin, J. E. Schirber, E. L. Venturini, and D. S. Ginley

*Sandia National Laboratories, Albuquerque, New Mexico 87185*

(Received 29 August 1988)

Superconducting samples of  $\text{La}_2\text{CuO}_{4+\delta}$  are shown by neutron powder diffraction to consist of two nearly identical orthorhombic phases. The primary phase has a stoichiometry near  $\text{La}_2\text{CuO}_4$ . The second phase is an oxygen-rich phase that is superconducting. The abundance of the second phase increases with the oxygen pressure at which the samples are annealed. Neutron-diffraction measurements as a function of temperature show that the phase separation occurs reversibly near 320 K.

### INTRODUCTION

At the time of the discovery of superconductivity at temperatures above 30 K in  $\text{La}_{2-x}\text{M}_x\text{CuO}_{4+\delta}$  ( $M = \text{Ba}$ ,  $x \approx 0.15$ ),<sup>1</sup> the parent compound  $\text{La}_2\text{CuO}_4$  that had been extensively studied for a number of years was thought to be nonmetallic.<sup>2-8</sup> Although some studies had not been extended to low temperature, those which had showed no superconducting behavior. Subsequent detailed studies of the effect of cation doping (for  $M = \text{Sr}$ ) on the superconducting properties showed that the superconducting transition temperature  $T_c$  initially increased with increasing doping, peaked near  $x = 0.15$ , and then decreased for further increases in  $x$ .<sup>9,10</sup> The undoped, semiconducting compound ( $x = 0$ ) was found to exhibit antiferromagnetic ordering on the Cu sites which has led to continuing investigations of the interplay between superconductivity and magnetism in these compounds.<sup>11</sup> All of these properties were observed to depend critically on the oxygen vacancy concentration which is controlled by the synthesis conditions.<sup>12</sup>

While further studies of the properties of nonsuperconducting  $\text{La}_2\text{CuO}_{4+\delta}$  were in progress, several laboratories unexpectedly reported the observation of traces of superconductivity with  $T_c$ 's between 30 and 40 K in undoped  $\text{La}_2\text{CuO}_{4+\delta}$  synthesized under slightly different conditions.<sup>13-15</sup> The superconducting samples were made by cooling slowly in oxygen, while rapid cooling produced semiconducting material. Meissner-effect measurements, however, showed superconducting fractions of less than 1%, making it impossible to conclude whether the observed superconductivity was an intrinsic property of  $\text{La}_2\text{CuO}_{4+\delta}$ . Working from the premise that increased oxygen content was the cause of the superconductivity, several laboratories employed methods to deliberately raise the oxygen stoichiometry. Tarascon *et al.* were able to insert oxygen by a low-temperature plasma-oxidation technique and achieve superconducting fractions as high as 18%.<sup>16</sup> Similar results were obtained in other laboratories by annealing  $\text{La}_2\text{CuO}_{4+\delta}$  in high static oxygen pressures at elevated temperatures.<sup>17-22</sup> For example, an-

nealing in 1-3 kbar of oxygen at 600 °C for 12-48 h followed by a 100 °C/h cooling resulted in superconducting fractions above 30%.<sup>20</sup> These experiments clearly established that bulk superconductivity could be achieved in  $\text{La}_2\text{CuO}_{4+\delta}$  by employing special synthesis conditions which were presumed to raise the oxygen content.

The general consensus from these studies is that metallic, superconducting behavior in  $\text{La}_2\text{CuO}_{4+\delta}$  results from the introduction of carriers when the oxygen stoichiometry is raised above the level required for formal charge balance. Several laboratories have attempted to establish whether the required charge imbalance results from the existence of La vacancies or the incorporation of more than four oxygen atoms per formula unit. Precedents for both possibilities occur in the same family of compounds. Up to 8% La vacancies have been reported in the related Co-containing compound, leading to the general formula  $\text{La}_{1.83}\text{CoO}_{4-\delta}$  ( $0 < \delta < 0.13$ ).<sup>23</sup> Conversely, in the  $\text{La}_2\text{NiO}_{4+\delta}$  system, recent structural and density studies have shown that extra oxygen (i.e.,  $\delta > 0$ ) can be introduced into the structure.<sup>24</sup>

In the case of  $\text{La}_{2-x}\text{CuO}_{4+\delta}$ , some variation in properties has been observed as a function of the initial La composition, but superconductivity has been observed over a wide range of bulk [La]:[Cu] ratios.<sup>10,25,26</sup> The subtle changes in bulk properties are thought to result from the presence of impurity phases. These results imply that the [La]:[Cu] ratio cannot be significantly varied. Schirber *et al.* performed careful electron microprobe analysis with an estimated uncertainty of 1% and measured a [La]:[Cu] ratio of 2:1 for a superconducting sample annealed in high-pressure oxygen.<sup>20</sup> A recent single-crystal neutron-diffraction study gave an overall stoichiometry of  $\text{La}_{1.998(4)}\text{Cu}_{0.050(3)}\text{Li}_{0.050(3)}\text{O}_{4.018(12)}$  for a crystal grown from a Li-containing flux (the refined Li content was in excellent agreement with chemical analysis), also suggesting that the existence of La vacancies is not the correct explanation for the charge imbalance.<sup>27</sup> Of course, the existence of vacancies on both the La and Cu sublattices is not ruled out (since no precise bulk density measurement has been made), but such an explanation seems unlikely.

In our own laboratory we have used multiphase Rietveld analysis of neutron-powder-diffraction data to carefully measure the abundance of CuO and La<sub>2</sub>O<sub>3</sub> impurity phases, and the structural parameters of the La<sub>2</sub>CuO<sub>4+δ</sub> primary phase, for a number of samples with different bulk (starting) compositions.<sup>28</sup> From our work, we conclude that the [La]:[Cu] ratio of La<sub>2</sub>CuO<sub>4+δ</sub> does not vary from 2:1 by more than 0.01. Thus, we conclude that no significant concentration of La vacancies is present and that superconductivity in La<sub>2</sub>CuO<sub>4+δ</sub> results from oxygen stoichiometries above 4.

Schirber *et al.* have determined the amount of excess oxygen in their superconducting samples by weight-gain and weight-loss measurements.<sup>20</sup> Superconducting samples annealed in 3 kbar of oxygen at 600 °C, which show superconducting fractions above 30%, reversibly lose 0.5% of their weight when annealed in vacuum at 500 °C for 0.5 h. Their as-prepared La<sub>2</sub>CuO<sub>4+δ</sub>, which shows traces of superconductivity, exhibits a 0.2% weight loss under the same conditions.<sup>20</sup> Iodometric titration also confirms that the superconducting sample contains excess oxygen leading to an increase in the amount of Cu<sup>3+</sup>. However, the titration results do not agree with the weight loss if the excess oxygen is assumed to be incorporated as O<sup>2-</sup>. A comparison of the weight loss and analytical results led to the conclusion that the excess oxygen is incorporated in the structure as a superoxide ion, O<sub>2</sub><sup>-</sup>, and that the approximate bulk stoichiometry of their superconducting sample was La<sub>2</sub>CuO<sub>4.13</sub>.<sup>20</sup> Recent x-ray photoemission studies by Rogers *et al.* support this superoxide assignment.<sup>21</sup> However, the existence of an oxygen-containing surface species in addition to excess bulk oxygen is also a possible explanation.

The neutron-diffraction studies reported in this paper were undertaken in an attempt to obtain structural evidence for the existence of excess oxygen in superconducting La<sub>2</sub>CuO<sub>4+δ</sub> and to learn the structure and location of the oxygen defect. Data were collected at both room temperature and low temperature in order to learn whether

the superconductivity might also be associated with a low-temperature structural phase transition in the oxygen-rich compound. We recently presented preliminary results that showed that additional Bragg peaks, appearing as shoulders on some of the orthorhombic La<sub>2</sub>CuO<sub>4+δ</sub> peaks, were visible at 10 K but not at room temperature.<sup>29</sup> In the present paper we report additional neutron-diffraction studies and detailed analyses which show that superconducting samples of La<sub>2</sub>CuO<sub>4+δ</sub> actually contain two closely-related orthorhombic phases whose Bragg peaks almost perfectly overlap. The second phase is observed only in samples which exhibit superconductivity and its abundance increases with the oxygen pressure at which the samples are annealed. Neutron-diffraction studies of a two-phase sample as a function of temperature show that the phase separation occurs reversibly near 320 K. The lattice parameters of the primary phase are nominally the same in single-phase and two-phase samples, suggesting that this phase is essentially stoichiometric La<sub>2</sub>CuO<sub>4.00</sub>. Since weight-loss measurements confirm that the two-phase samples have overall oxygen concentrations significantly greater than 4, we conclude that the second phase is an oxygen-rich form of La<sub>2</sub>CuO<sub>4+δ</sub> that is superconducting.

#### SAMPLE PREPARATION AND CHARACTERIZATION

Samples for these studies were prepared by two different techniques. A summary of the six samples studied by neutron powder diffraction is given in Table I. At Sandia, La<sub>2</sub>CuO<sub>4+δ</sub> samples were prepared by grinding stoichiometric mixtures of La<sub>2</sub>O<sub>3</sub> and CuO powders in an agate mortar and sintering in air for 45 h at 1100 °C followed by a 900 °C oxygen anneal for 12 h and a 5 h slow cool in oxygen.<sup>20,21,29</sup> These as-prepared samples exhibited traces of superconductivity (zero resistance near 30 K) with the superconducting fraction, as measured by low-field flux exclusion at 5 K, varying from 0.2% to 0.5% depending on the size of the initial fired ceramic. Bulk superconducting samples were then made from this material

TABLE I. Summary of samples studied by neutron powder diffraction.  $T_c$  is the resistive onset temperature for the superconducting transition. The percentage of *Fmmm* phase is determined by two-phase Rietveld refinement of neutron-powder-diffraction data taken at 10 K. The range of values listed for two of the samples results from the use of different structural models (see text). The superconducting (SC) fraction is determined by low-field flux-exclusion measurements at 5 K. The weight loss is the change in weight resulting from annealing in vacuum or flowing nitrogen. The bulk oxygen content is calculated from the weight loss, assuming that the vacuum- or nitrogen-annealed samples have a stoichiometry of La<sub>2</sub>CuO<sub>4.00</sub>.

Sample	$T_c$ (K)	<i>Fmmm</i> phase (%)	SC fraction (%)	Wt. loss (%)	Oxygen content
Sandia, 3-kbar	34	53–60	30	0.5	4.13
Argonne, 0.1-kbar	38	27–30	0.2–0.5	0.1	4.03
Sandia, as-prepared	38	12	0.2–0.5	0.03–0.2 <sup>a</sup>	4.01–4.05 <sup>a</sup>
Argonne, as-prepared	38	8	0.01	0.03	4.01
Sandia, vacuum-annealed	0	< 4	0	0	4.00
Argonne, nitrogen-annealed	0	< 4	0	0	4.00

<sup>a</sup>Vacuum and nitrogen annealing give different weight losses for different samples.

by annealing in 3 kbar of oxygen at 600°C for 12 h followed by a 100°C/h cool in the pressure cell after which the pressure was released. This technique resulted in samples which showed superconducting fractions above 30%. Since the volume of the pressure cell limited the sample size to about 150 mg, several high-pressure runs were required to achieve a 0.6-g sample for the neutron-diffraction studies.

At Argonne,  $\text{La}_2\text{CuO}_{4+\delta}$  samples were prepared by sintering the mixed and wet-ball-milled oxide powders at 975°C in oxygen for 12 h followed by a 10-h cool to room temperature. Again, these as-prepared samples showed traces of superconductivity with  $T_c$  (resistive onset) near 38 K, with the superconducting fraction as measured by low-field flux exclusion at 5 K near 0.01%. These samples were then annealed in 0.1 kbar of oxygen at 580°C for 48 h followed by a 24-h cool to room temperature. Care was taken to prevent possible water contamination which frequently occurs in closed systems. Thus, before the high-pressure annealing, the pressure cell was heated to 580°C and purged with flowing dry oxygen for 24 h. The resulting samples showed well-defined resistive transitions and the superconducting fraction was increased to 0.2–0.5%. Samples with trace amounts of superconductivity tend to show differences in the superconducting fraction depending on sample preparation and morphology.

The systematic difference in the size of the superconducting fraction, as measured by low-field flux exclusion, for the Argonne samples versus the Sandia samples is thought to result from two effects. Scanning electron microscopy shows that the Argonne as-prepared material has an average grain size near 3  $\mu\text{m}$ , while in the Sandia as-prepared material the grain size is 15–20 times larger. Additionally, as will be discussed in more detail later, the neutron-diffraction data show that the domains of superconducting phase in the Argonne 0.1-kbar sample have dimensions near 3000 Å, while the domains of superconducting phase in the Sandia 3-kbar sample are much larger. Since the magnetic penetration depth is estimated to be 2000–2500 Å,<sup>30,31</sup> it is not surprising that the Argonne samples exhibit unusually small flux exclusion and Meissner effects even though they contain significant amounts of the superconducting phase. Although the fraction of superconducting phase in the Argonne 0.1-kbar sample (30% from neutron diffraction) was not as high as that produced in the Sandia sample by annealing in 3 kbar of oxygen (60% from neutron diffraction), the 0.1-kbar oxygen-annealing technique allowed the synthesis of large (10 g) samples of superconducting  $\text{La}_2\text{CuO}_{4+\delta}$  which could be used for rapid collection of high-quality neutron-powder-diffraction data over a range of temperatures. This ability to maximize counting statistics proved to be especially important for obtaining diffraction data from which two distinct phases could be identified.

For each sample, the total excess oxygen was estimated by weight-loss measurements. The sample masses were measured before and after annealing in vacuum or flowing nitrogen at 600°C. This anneal in vacuum or nitrogen destroys all traces of superconductivity. These vacuum- or nitrogen-annealed samples were also studied by neutron diffraction, for comparison with the neutron-

diffraction results from the as-prepared and high-pressure-oxygen-annealed samples. In order to establish a reference for the weight-loss measurements, the oxygen content of a nitrogen-annealed sample was determined by hydrogen reduction, yielding a stoichiometry of  $\text{La}_2\text{CuO}_{3.992}$ . Thus, within our ability to measure, the vacuum or nitrogen-annealed samples are stoichiometric. Based on this reference, the weight-loss measurements can be used to calculate the total oxygen content for each sample. The calculated bulk compositions are listed along with the measured weight losses in Table I. Since  $\text{La}_2\text{CuO}_{4+\delta}$  samples are observed to be quite reactive, and adsorbed water or other surface species can contribute to the observed weight loss, these values should be taken as upper bounds for the actual compositions.

### NEUTRON-POWDER-DIFFRACTION MEASUREMENTS

Neutron-powder-diffraction data were collected at both room temperature and 10 K for the six samples listed in Table I using the Special Environment Powder Diffractometer<sup>32,33</sup> at Argonne's Intense Pulsed Neutron Source. For low-temperature data collection, the samples were sealed along with 1 atm of helium exchange gas in thin-walled vanadium cans and cooled by a closed-cycle helium (Displex) refrigerator. For the Argonne sample processed in 0.1 kbar of oxygen, additional data were collected for a number of temperatures between 10 K and room temperature using the Displex refrigerator and also from room temperature to 498 K using two different furnaces.

In the raw data at 10 K for the two superconducting samples annealed in high-pressure oxygen, new Bragg peaks were clearly visible as shoulders on some of the Bragg peaks of the known orthorhombic  $\text{La}_2\text{CuO}_{4+\delta}$  structure. In our previous paper, based on data from only the Sandia sample we were unable to conclude whether these new peaks resulted from a subtle structural distortion or from the existence of a second phase.<sup>29</sup> The additional data from the Argonne sample, which had a smaller fraction of the superconducting phase but provided better counting statistics, showed that the intensities of the new peaks scaled together, leading directly to the conclusion that two distinct phases were present. This two-phase behavior can be clearly seen in Fig. 1, which shows a portion of the diffraction pattern for samples with three different concentrations of the second phase.

Since no new Bragg peaks were observed except for those on the shoulders of existing peaks, an initial Rietveld structural refinement<sup>34</sup> based on a mixture of two orthorhombic *Bmab* phases was attempted for the Argonne 0.1-kbar sample at 10 K. This refinement immediately converged to a low-*R* value and yielded lattice constants for the two phases which agreed with all of the observed reflections. However, based on the refined lattice constants it was clear that a small number of weak reflections for the second phase which should have been almost completely resolved were systematically absent. Specifically, the 014, 121, and 032 reflections were not observed for the second phase. The lack of intensity in these reflections indicates that the nearly rigid tilt of the  $\text{CuO}_6$  octahedra

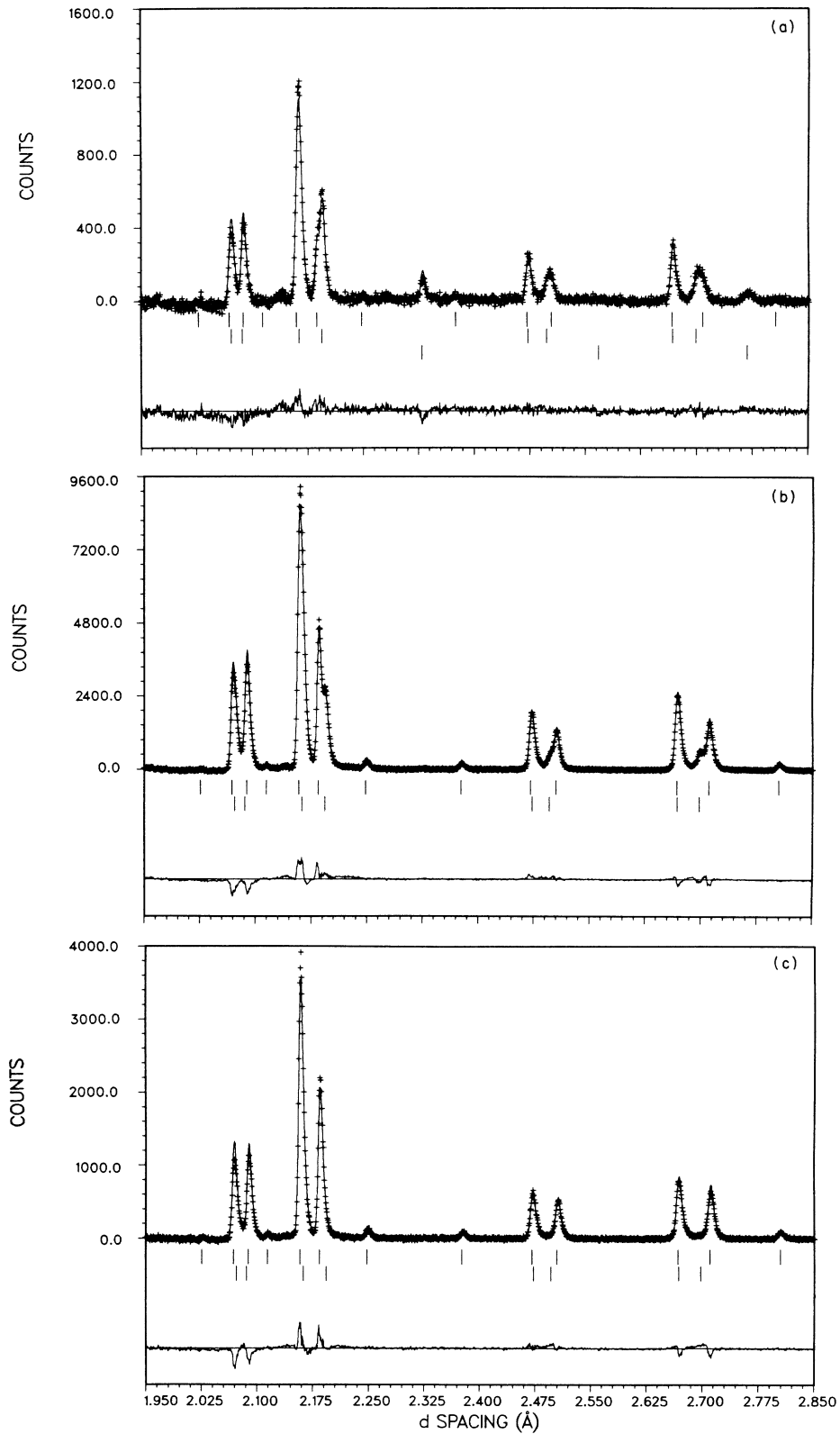


FIG. 1. Portion of the Rietveld refinement profile for the (a) Sandia 3-kbar, (b) Argonne 0.1-kbar, and (c) Argonne nitrogen-annealed  $\text{La}_2\text{CuO}_{4+\delta}$  samples (see Table I) analyzed with a two-phase model. Plus marks (+) are the raw data. The solid line is the calculated profile. Tick marks below the diffraction profile indicate the positions of allowed reflections in the model. The upper row of tick marks is for the orthorhombic *Bmab* phase; the second row is for the orthorhombic *Fmmm* phase. In the case of the Sandia 3-kbar sample a third row of tick marks indicates the position of allowed reflections from cadmium which is used to mask the sample container. A difference curve (observed minus calculated) is plotted at the bottom. Background has been subtracted prior to plotting.

( $\sim 5^\circ$  and 10 K) present in the orthorhombic,  $Bmab$ ,  $\text{La}_2\text{CuO}_{4+\delta}$  structure<sup>7</sup> is not present in the structure of the second phase, and requires either an accidental combination of atom positions in the  $Bmab$  space group, giving rise to the zero intensities, or that the space group of the second phase is  $F$  centered. In the initial refinement based on two  $Bmab$  phases, the expected rigid tilt of the  $\text{CuO}_6$  octahedra was observed for the primary phase (see Table II), but for the second phase the refinement yielded opposing directions for the  $\text{O}(1)$  and  $\text{O}(2)$  displacements, defining an unusual distortion of the octahedra rather than a rigid tilt. Thus, subsequent refinements based on one  $Bmab$  phase and one  $F$ -centered phase were attempted.

Three space groups are allowed by the observed  $(h+k, k+l, h+l=2n)$  extinctions— $Fmmm$ ,  $Fmm2$ , and  $F222$ .  $Fmm2$  is a polar space group which allows independent values of  $z$  for  $\text{O}(2)$  at  $(0,0,z)$  and  $(0,0,-z)$  and allows  $\text{Cu}$  to be displaced from the center of the  $\text{CuO}_6$  octahedron along  $z$ . Attempted refinements using an  $Fmm2$  model for phase two were unstable.

The  $F222$  space group requires  $\text{O}(2)$  to be on the special position  $(0,0,z)$  but allows  $\text{O}(1)$  to be displaced into a site of twofold symmetry. Thus, the four  $\text{O}(1)$  atoms around the  $\text{Cu}$  atom at  $(0,0,0)$  have the positions  $(\frac{1}{4}, \frac{1}{4}, z)$ ,  $(\frac{3}{4}, \frac{3}{4}, z)$ ,  $(\frac{1}{4}, \frac{3}{4}, -z)$ , and  $(\frac{3}{4}, \frac{1}{4}, -z)$ . If an anisotropic temperature factor is allowed for  $\text{O}(2)$ , this model also yields low- $R$  values. However, if an anisotropic temperature factor is also used for  $\text{O}(1)$ , the thermal ellipsoid becomes elongated along the  $z$  axis and the static displacement,  $z(\text{O}(1))$ , converges toward zero. As

$z(\text{O}(1))$  approaches zero, correlations between  $z(\text{O}(1))$  and  $B_{33}(\text{O}(1))$  become high and the refinement becomes unstable. This result suggests again that static displacements are present, but that they do not obey the symmetry required by the  $F222$  space group. Moreover, for  $z(\text{O}(1))=0$  the  $F222$  space group becomes equivalent to the  $Fmmm$  space group.

In space group  $Fmmm$  the oxygen atoms must both be placed on special positions,  $\text{O}(1)$  at  $(\frac{1}{4}, \frac{1}{4}, 0)$  and  $\text{O}(2)$  at  $(0,0,z)$ , or they must be disordered. Refinements with both oxygen atoms on special positions, with isotropic temperature factors, yielded higher  $R$  values than for the  $Bmab$  model. However, when anisotropic temperature factors were used, the  $R$  value was substantially lowered. Of the models investigated, this model yielded the lowest  $R$  values. The thermal ellipsoids were elongated along  $z$  for  $\text{O}(1)$  and perpendicular to  $z$  for  $\text{O}(2)$ , suggesting that rather large displacements are present. Since the data were taken at 10 K, these displacements are assumed to be static, not thermal.

The overall conclusion from these attempted refinements is that it is impossible to uniquely differentiate between  $Bmab$ ,  $Fmmm$ , and  $F222$  models for phase two. This inability to establish a unique structure is compounded by the fact that phase two must contain excess oxygen as a defect which has not been included in the refinement model. As might be expected for two-phase data where the corresponding peaks from the two phases are heavily overlapped, attempts to test various defect models were also inconclusive. The defect proposed by Buttrey *et al.* for oxygen-rich  $\text{La}_2\text{NiO}_{4+\delta}$  in which an  $\text{O}(2)$  atom is re-

TABLE II. Structural parameters at 10 K determined from a two-phase Rietveld refinement of neutron-powder-diffraction data for the orthorhombic  $Bmab$  and  $Fmmm$  phases of the samples indicated. (See text and Table I for a more complete description of the samples.) Numbers in parentheses are standard deviations of the last significant digit.

$R_{wp}/R_{exp}$	Sandia 3-kbar sample 0.0412/0.0307		Argonne 0.1-kbar sample 0.0437/0.0178		Argonne nitrogen-annealed sample 0.0476/0.0289
	$Bmab$ phase	$Fmmm$ phase	$Bmab$ phase	$Fmmm$ phase	$Bmab$ phase
$a$ (Å)	5.3337(3)	5.3346(3)	5.3350(1)	5.3364(2)	5.3349(1)
$b$ (Å)	5.4143(3)	5.3969(3)	5.4209(1)	5.3955(2)	5.4204(1)
$c$ (Å)	13.1258(7)	13.1646(7)	13.1068(2)	13.1615(5)	13.1072(1)
$V$ (Å <sup>3</sup> )	379.053(20)	379.019(19)	379.058(6)	378.952(15)	379.025(5)
La					
$x$	0	0	0	0	0
$y$	-0.0088(8)	0	-0.0095(2)	0	-0.0092(2)
$z$	0.3620(3)	0.3601(3)	0.3618(1)	0.3604(2)	0.3616(1)
$B$ (Å <sup>2</sup> )	-0.08(8)	0.38(10)	0.00(2)	0.19(5)	0.01(1)
Cu					
$x=y=z$	0	0	0	0	0
$B$ (Å <sup>2</sup> )	0.05(11)	-0.02(11)	-0.06(3)	0.10(7)	-0.06(2)
$\text{O}(1)$					
$x=y$	$\frac{1}{4}$	$\frac{1}{4}$	$\frac{1}{4}$	$\frac{1}{4}$	$\frac{1}{4}$
$z$	0.0086(4)	0	0.0085(1)	0	0.0087(1)
$B$ (Å <sup>2</sup> )	0.03(9)	0.82(12)	0.12(2)	0.68(7)	0.15(2)
$\text{O}(2)$					
$x$	0	0	0	0	0
$y$	0.0437(8)	0	0.0426(2)	0	0.0410(2)
$z$	0.1842(5)	0.1845(6)	0.1839(1)	0.1828(4)	0.1841(1)
$B$ (Å <sup>2</sup> )	-0.22(8)	1.93(13)	0.11(2)	1.50(7)	0.21(2)
Scale factor	0.165(12)	0.189(14)	1.84(2)	0.779(14)	0.885(3)

placed by an O-O dumbbell,<sup>24</sup> does refine successfully. However, an alternate model involving interstitial O<sup>2-</sup> in the La-O layer also refines. Thus, it is impossible to demonstrate uniqueness. One general conclusion that can be drawn is that phase two is a structure in which the oxygen-atom displacements, which lead to a rigid tilt of the linked CuO<sub>6</sub> octahedra in the *Bmab* phase, have been disordered into random directions. Perhaps this frustration of the coordinated tilting, which requires some octahedra to be distorted, is a result of the oxygen defect that must be present in phase two. It should also be noted that defect ordering could result in the formation of a supercell with superlattice reflections too weak to observe in the present study.

Realizing that a unique solution for the structure of phase two could not be obtained, subsequent two-phase refinements were done with an *Fmmm* model (with isotropic temperature factors) for the second phase. The refined parameters for the *Bmab* and *Fmmm* phases for the Sandia 3-kbar and Aronne 0.1-kbar samples and the *Bmab* phase of the Argonne nitrogen-annealed sample at 10 K are given in Table II. Figure 1 shows a portion of the Rietveld refinement profile for the same three refinements.

Two-phase Rietveld refinements based on a mixture of orthorhombic *Bmab* and orthorhombic *Fmmm* phases were performed for all of the samples listed in Table I in order to determine the relative fractions of the two phases in each sample and the structural parameters of each phase. Since the lattice parameters of the two phases are more widely separated at low temperature, conclusions concerning the relative fractions of the two phases were based on data collected at 10 K. In these two-phase refinements the refined parameters included the lattice parameters, atom positions, isotropic temperature factors, isotropic peak widths, and overall scale factors for each phase. Due to high correlations (presumably resulting from the extensive peak overlap), refinements in which the oxygen site occupancies of both phases were varied were found to be marginally unstable, leading to unreliable values for these parameters. Thus, oxygen site occupancies were fixed at their ideal values.

The relative fractions of the two phases for each sample are listed in Table I. The Sandia sample annealed at 3-kbar oxygen pressure is approximately 60% *Fmmm* phase and 40% *Bmab* phase. (The phase fraction given by the refinement varies somewhat depending on whether isotro-

pic or anisotropic temperature factors are used in the structural model and on the form of absorption and extinction corrections applied to the data.) The Argonne sample annealed at 0.1-kbar oxygen pressure is 30% *Fmmm* phase. The Sandia and Argonne as-prepared samples contain 12% and 8% of the *Fmmm* phase, respectively. Two-phase Rietveld refinements for samples annealed in vacuum or nitrogen yield values of less than 4% for the *Fmmm* phase (if the structural parameters for the *Fmmm* phase are held constant). Since, in this case, attempts to refine only the lattice parameters of the *Fmmm* phase lead to unphysical values, we conclude that the small improvement in fit offered by the two-phase model for these samples is not valid evidence for the presence of the *Fmmm* phase. Thus, the limit of detectability for the *Fmmm* phase by this technique is apparently near 4%, and we have no evidence that the vacuum- or nitrogen-annealed samples contain any *Fmmm* phase.

The lattice parameters for the *Bmab* and *Fmmm* phases for each of the samples at 10 K are given in Table III. The *c* axis of the *Fmmm* phase is systematically larger than that of the *Bmab* phase by about 0.4%. This lengthening of the *c* axis is compensated by a shortening of the *b* axis, such that the cell volumes of the two phases are nominally the same. Much smaller changes in lattice parameters are observed within a given phase, suggesting that the stoichiometry of the *Bmab* (or *Fmmm*) phase is nearly the same in all samples. In particular, the *Bmab* phase in two-phase (superconducting) samples is essentially the same as the *Bmab* phase observed in the vacuum- or nitrogen-annealed samples for which our hydrogen-reduction experiment gave nearly perfect stoichiometry. From this result we conclude that the *Bmab* phase in these six samples always has a stoichiometry near La<sub>2</sub>CuO<sub>4</sub>. Thus, the excess oxygen is almost entirely incorporated into the *Fmmm* phase. This conclusion is, of course, consistent with the concept of phase separation and implies that the separation process involves long-range oxygen diffusion which leads to domains of a defect-ed (oxygen-rich) phase and an undefected phase.

The domain size can, in principle, be estimated from the width of the diffraction peaks. With the time-of-flight method, the peak-broadening effects of strains and particle (domain) size can be differentiated because they have different wavelength dependence. For strain broadening,  $\Delta d/d$  is a constant (where *d* is the plane spacing). For particle-size broadening,  $\Delta d/d = Cd/D$ , where  $C \approx 1$  and

TABLE III. Refined lattice parameters and cell volumes at 10 K for the six La<sub>2</sub>CuO<sub>4+ $\delta$</sub>  samples studied by neutron powder diffraction. Numbers in parentheses are statistical standard deviations of the last significant digit. Due to correlations in the two-phase refinement, the actual uncertainties are much larger.

Sample	<i>Bmab</i> phase				<i>Fmmm</i> phase			
	<i>a</i> (Å)	<i>b</i> (Å)	<i>c</i> (Å)	<i>V</i> (Å <sup>3</sup> )	<i>a</i> (Å)	<i>b</i> (Å)	<i>c</i> (Å)	<i>V</i> (Å <sup>3</sup> )
Sandia, 3-kbar	5.3337(3)	5.4143(3)	13.1258(7)	379.06	5.3346(3)	5.3969(2)	13.1646(7)	379.02
Argonne, 0.1-kbar	5.3350(1)	5.4209(1)	13.1068(2)	379.06	5.3364(2)	5.3955(2)	13.1615(5)	378.95
Sandia, as-prepared	5.3340(1)	5.4199(1)	13.1115(1)	379.05	5.3351(5)	5.3933(4)	13.1693(12)	378.93
Argonne, as-prepared	5.3347(1)	5.4212(1)	13.1058(1)	379.03	5.3427(4)	5.3929(4)	13.1520(11)	378.94
Sandia, vacuum-annealed	5.3340(1)	5.4203(1)	13.1094(1)	379.02				
Argonne, nitrogen-annealed	5.3349(1)	5.4204(1)	13.1072(1)	379.03				

$D$  is the dimension of the particle. Since the resolution of the special environment powder diffractometer is  $\Delta d/d \approx 0.0035$ , particle-size peak-broadening effects can be readily measured for particles of dimensions less than about 5000 Å. For the refinements of the six  $\text{La}_2\text{CuO}_{4+\delta}$  samples, no significant particle-size peak broadening was observed for the  $Bmab$  phase of any of the samples. For the  $Fmmm$  phase, peak broadening could only be accurately modeled in the two high-pressure-annealed samples where the phase fractions were 30% and 60% (see Table I). The  $Fmmm$  phase in the Argonne 0.1-kbar sample showed particle-size peak broadening equivalent to an average particle dimension of about 3000 Å. This observation is consistent with the concept of a phase separation in which the  $Fmmm$  phase nucleates and grows in a matrix of the  $Bmab$  primary phase. Even though 30% of this sample is in the superconducting phase, the domains are sufficiently small in comparison to the magnetic penetration depth [2000–2500 Å (Refs. 30 and 31)] that Meissner-effect and flux-exclusion measurements yield small values. Conversely, the  $Fmmm$  phase in the Sandia 3-kbar sample showed no measurable peak broadening. This is consistent with a much larger domain size. Moreover, with 60% of the sample being in the  $Fmmm$  phase, the majority of domains must have merged. Both of these effects would lead to the substantially larger superconducting fraction (30%) as measured by flux exclusion (see Table I). From these two samples it is impossible to determine whether the density of nucleation centers is the same in the Argonne and Sandia samples. Differences arising from the different sample preparation techniques are certainly possible and could explain the variation in superconducting fractions for the as-prepared samples listed in Table I.

#### TEMPERATURE DEPENDENCE OF THE PHASE SEPARATION

In an attempt to further understand the phase-separation process, the Argonne sample annealed in 0.1 kbar of oxygen was studied at a number of temperatures from 10 to 498 K. A full Rietveld refinement was performed on each data set in order to determine the relative fraction and the structural parameters of the two phases. The results of these studies are summarized in Fig. 2, where the lattice parameters are plotted as a function of temperature.

The phase separation occurs at about 320 K. All data below this temperature can be successfully refined with a two-phase model. For this study, the sample is assumed to be single phase when we can no longer resolve a difference between the refined lattice constants of the two phases and when  $R$  value ratio tests favor a single-phase refinement model. The fraction of  $Fmmm$  phase remains constant at 30%, within the experimental error of 1%, over the temperature range from 10 to 320 K, with the qualification that the phase fraction must be fixed as the lattice constants converge near the phase-separation temperature. It is not clear from these results whether the discontinuity of the  $a$  lattice constant for the  $Fmmm$  phase near the

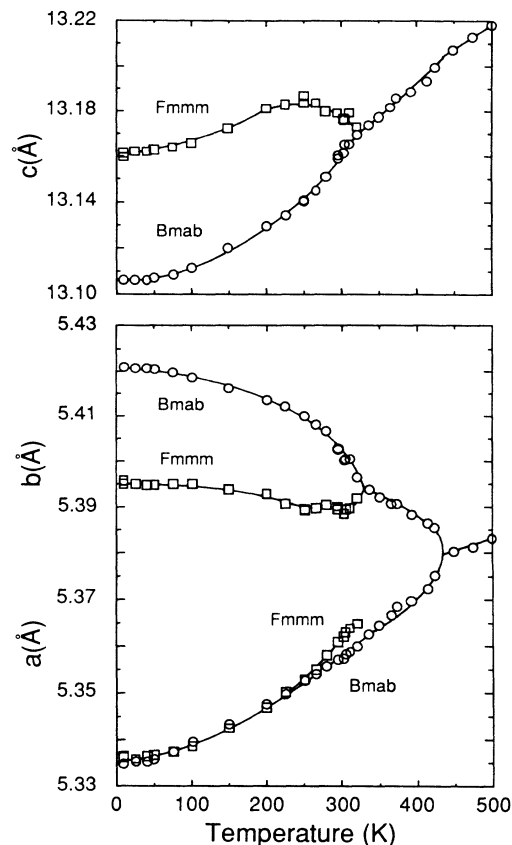


FIG. 2. Lattice constants vs temperature for the Argonne  $\text{La}_2\text{CuO}_{4+\delta}$  sample processed in 0.1 kbar of oxygen at 580°C. From 10 to 320 K the data are refined with a two-phase model based on orthorhombic  $Bmab$  and  $Fmmm$  phases. From 320 to 430 K a single  $Bmab$  phase is observed. Above 430 K the structure is tetragonal  $I4/mmm$ .

phase-separation temperature is real or is an artifact of the data analysis. Such a discontinuity in lattice constants would, in general, be expected for the minor phase in a phase-separation process depending on the detailed shape of the phase diagram. However, anomalies in the refined lattice constants could also result from anisotropic peak broadening (which we have not attempted to model) associated with a decreasing domain size in this temperature region near the phase separation. Overall, however, the two-phase refinements near the phase-separation temperature are surprisingly stable.

Immediately above the phase separation at 320 K, the sample is single-phase orthorhombic with the  $Bmab$  structure. Changes in the thermal expansion (especially along the  $b$  and  $c$  axes) of the  $Bmab$  phase in this single-phase region (Fig. 2) undoubtedly result from the small concentration of excess oxygen which must be present as a defect in the single-phase region. The orthorhombic strain ( $b-a$ ) decreases with increasing temperature until a transition to the tetragonal  $I4/mmm$  structure occurs near 430 K. This orthorhombic-to-tetragonal structural transition in  $\text{La}_2\text{CuO}_{4+\delta}$  was previously reported to occur at temperatures ranging from 450 to 530°C, and is known to depend critically on the oxygen stoichiometry of the sample.<sup>12</sup> There

is no precedent in the literature for predicting the transition temperature for a sample with oxygen stoichiometry above 4. However, the lowering of the transition temperature for an oxygen-rich sample is in qualitative agreement with the data of Johnston *et al.*<sup>12</sup>

The behavior shown in Fig. 2 was found to be completely reversible. The high-temperature data were taken in two separate experiments in different furnaces. In the first experiment, data were collected to a maximum temperature of 413 K. Subsequent Rietveld analysis showed that we had not quite reached the tetragonal phase. Thus, in the second experiment, a small number of points were taken within the previous temperature range and the maximum temperature was extended to 498 K. After each high-temperature experiment, data were collected at 10 K. In both cases, analysis of the 10-K data gave the same relative phase fraction (30%) and the same lattice constants for the two phases, implying that there had been no loss of oxygen during the high-temperature experiments.

#### DISCUSSION AND CONCLUSIONS

These results show that samples of  $\text{La}_2\text{CuO}_{4+\delta}$  which exhibit superconducting behavior contain two closely-related orthorhombic phases. Samples prepared by various techniques all contain the previously reported *Bmab* orthorhombic phase with only small variations in lattice constants. This phase is concluded to be nominally stoichiometric  $\text{La}_2\text{CuO}_4$  based on a hydrogen reduction of one of the single-phase (nitrogen-annealed) samples. For the six samples examined in this study, a second orthorhombic phase (analyzed in space group *Fmmm*) is always present when superconductivity is observed, and is not observed in nonsuperconducting samples. The two-phase behavior is the result of a macroscopic phase separation which occurs near 320 K. Since the overall oxygen content of the superconducting samples is measured to be greater than 4, this second phase is concluded to be an oxygen-rich phase whose superconducting properties arise from the charge imbalance provided by the excess oxygen.

The structure of the superconducting phase is closely related to the nonsuperconducting *Bmab*  $\text{La}_2\text{CuO}_4$  phase and may in fact belong to the same space group. The largest difference in lattice parameters is 0.4% and occurs at low temperature (< 200 K). The failure to observe intensity in a small number of resolved reflections suggest that the actual structure is *F*-centered (probably *Fmmm* or *F222*), but extensive overlap of the diffraction peaks makes a unique determination of the structure impossible.

Additionally, it is not possible to determine the structure of the oxygen defect by which the excess oxygen is accommodated. For these reasons, more detailed conclusions concerning the temperature- and/or oxygen-composition phase diagram are not possible. If both phases are *Bmab*, the phase diagram could involve a classic miscibility gap. However, if the structures are different, the phase diagram must be more complex.

For some samples which contain large fractions of the superconducting phase, the measured Meissner effect and flux exclusion remain small because the superconducting domain size is of the order of the magnetic penetration depth. However, as the fraction of the superconducting phase is increased further (by annealing at higher oxygen pressures) the domains grow and become connected and large Meissner effects are observed.

With the oxygen pressures employed in this study it has not been possible to make samples entirely in the superconducting phase. Thus, for these samples, the oxygen concentration in the superconducting phase is controlled only by the shape of the phase diagram (which may itself have some pressure dependence). Within the pressure range we have employed, annealing at different oxygen pressures changes only the relative fraction of the superconducting and nonsuperconducting phases. This phase-separation model is, therefore, consistent with our observation (Table I), and various reports in the literature, that superconducting  $\text{La}_2\text{CuO}_{4+\delta}$  exhibits surprising little variation in the transition temperature  $T_c$ .

*Note added in proof.* After this paper was accepted for publication we became aware of the synthesis of bulk superconducting  $\text{La}_2\text{CuO}_{4+\delta}$  at 800 °C and 23 kbar oxygen pressure.<sup>35</sup> In agreement with our results, those authors conclude that superconductivity results from excess bulk oxygen ( $\delta \approx 0.05$ ) incorporated as an  $\text{O}^{2-}$  interstitial defect (whose structure has not been determined), and that an additional superficial oxygen-containing species can produce misleading TGA and XPS results and overestimates of the value of  $\delta$ .

#### ACKNOWLEDGMENTS

This work is supported at Argonne National Laboratory by the U.S. Department of Energy, Basic Energy Sciences—Materials Sciences, under Contract No. W-31-109-ENG-38, and at Sandia National Laboratories by the U.S. Department of Energy under Contract No. DE-AC04-76DP00789.

<sup>1</sup>J. G. Bednorz and K. A. Müller, *Z. Phys. B* **64**, 198 (1986); S. Uchida, H. Takagi, K. Kitazawa, and S. Tanaka, *Jpn. J. Appl. Phys.* **26**, L1 (1987); H. Takagi, S. Uchida, K. Kitazawa, and S. Tanaka, *ibid.* **26**, L123 (1987).

<sup>2</sup>J. M. Longo and P. M. Raccach, *J. Solid State Chem.* **6**, 526 (1973).

<sup>3</sup>P. Ganguly and C. N. R. Rao, *Mater. Res. Bull.* **8**, 405 (1973).

<sup>4</sup>J. B. Goodenough, *Mater. Res. Bull.* **8**, 423 (1973).

<sup>5</sup>R. Saez-Puche, M. Norton, and W. S. Glausinger, *Mater. Res. Bull.* **17**, 1429 (1982).

<sup>6</sup>K. K. Singh, P. Ganguly, and J. B. Goodenough, *J. Solid State Chem.* **52**, 254 (1984).

<sup>7</sup>J. D. Jorgensen, H. B. Schuttler, D. G. Hinks, D. W. Capone II, K. Zhang, M. B. Brodsky, and D. J. Scalapino, *Phys. Rev. Lett.* **58**, 1024 (1987).

<sup>8</sup>S. Uchida, H. Takagi, H. Yanagisawa, K. Kishio, K. Kitazawa, K. Fueki, and S. Tanaka, *Jpn. J. Appl. Phys.* **26**, L445 (1987); T. Fujita, Y. Aoki, Y. Maeno, J. Sakurai, H. Fukuba, and H. Fujii, *ibid.* **26**, L368 (1987).

<sup>9</sup>R. B. van Dover, R. J. Cava, B. Batlogg, and E. A. Rietman,

- Phys. Rev. B **35**, 5337 (1987).
- <sup>10</sup>D. G. Hinks, B. Dabrowski, K. Zhang, C. U. Segre, J. D. Jorgensen, L. Soderholm, and M. A. Beno, in *High-Temperature Superconductors*, edited by M. B. Brodsky, R. C. Dynes, K. Kitazawa, and H. L. Tuller, Mater. Res. Soc. Symp. Proc. Vol. 99 (Materials Research Society, Pittsburgh, PA, 1988), p. 9.
- <sup>11</sup>D. Vaknin, S. K. Sinha, D. E. Moncton, D. C. Johnston, J. M. Newsam, C. R. Safinya, and H. E. King, Jr., Phys. Rev. Lett. **58**, 2802 (1987). For a recent review, see S. K. Sinha, Mater. Res. Soc. Bull. **13**, 24 (1988).
- <sup>12</sup>D. C. Johnston, J. P. Stokes, D. P. Goshorn, and J. T. Lewandowski, Phys. Rev. B **36**, 4007 (1987).
- <sup>13</sup>P. M. Grant, S. S. P. Parkin, V. Y. Lee, E. M. Engler, M. L. Ramirez, G. Lim, and R. D. Jacowitz, Phys. Rev. Lett. **58**, 2482 (1987).
- <sup>14</sup>J. Beille, R. Cabanel, C. Chaillout, B. Chevalier, G. Demazeau, F. Deslandes, J. Etourneau, P. Lejay, C. Michel, J. Provost, B. Raveau, A. Sulpice, J.-L. Tholence, and R. Tournier, C. R. Acad. Sci. Ser. 2 **304**, 1097 (1987).
- <sup>15</sup>K. Sekizawa, Y. Takano, H. Takigami, S. Tasaki, and T. Inaba, Jpn. J. App. Phys. **26**, L840 (1987).
- <sup>16</sup>J. M. Tarascon, L. H. Greene, B. G. Bagley, W. R. McKinnon, P. Barboux, and G. W. Hull, in *Novel Superconductivity*, edited by S. A. Wolf and V. Z. Kresin (Plenum, New York, 1987), pp. 705–724.
- <sup>17</sup>J. Beille, B. Chevalier, G. Demazeau, F. Deslandes, J. Etourneau, O. Laborde, C. Michel, P. Lejay, J. Provost, B. Raveau, A. Sulpice, J. L. Tholence, and R. Tournier, Physica B **146**, 307 (1987).
- <sup>18</sup>J. L. Tholence, Physica B **148**, 353 (1987).
- <sup>19</sup>J. E. Schirber, E. L. Venturini, B. Morosin, J. F. Kwak, D. S. Ginley, and R. J. Baughman, in *High-Temperature Superconductors*, edited by M. B. Brodsky, R. C. Dynes, K. Kitazawa, and H. L. Tuller, Mater. Res. Soc. Symp. Proc. Vol. 99 (Materials Research Society, Pittsburgh, PA, 1988), pp. 479–481.
- <sup>20</sup>J. E. Schirber, B. Morosin, R. M. Merrill, P. F. Hlava, E. L. Venturini, J. F. Kwak, P. J. Nigrey, R. J. Baughman, and D. S. Ginley, Physica C **152**, 121 (1988).
- <sup>21</sup>J. W. Rogers, Jr., N. D. Shinn, J. E. Schirber, E. L. Venturini, D. S. Ginley, and B. Morosin, Phys. Rev. B **38**, 5021 (1988).
- <sup>22</sup>G. Demazeau, F. Tresse, Th. Plante, B. Chevalier, J. Etourneau, C. Michel, H. Hervieu, B. Raveau, P. Lejay, A. Sulpice, and R. Tournier, Physica C **153-155**, 824 (1988).
- <sup>23</sup>J. T. Lewandowski, R. A. Beyerlein, J. M. Longo, and R. A. McCauley, J. Am. Ceram. Soc. **69**, 699 (1986).
- <sup>24</sup>D. J. Buttrey, P. Ganguly, J. M. Honig, C. N. R. Rao, R. R. Schartman, and G. N. Subbanna, J. Solid State Chem. **74**, 233 (1988).
- <sup>25</sup>S. M. Fine, M. Greenblatt, S. Simizu, and S. A. Friedberg, Phys. Rev. B **36**, 5716 (1987).
- <sup>26</sup>S. A. Shaheen, N. Jisrawi, Y. H. Lee, Y. Z. Zhang, M. Croft, W. L. McLean, H. Zhen, L. Rebelsky, and S. Horn, Phys. Rev. B **36**, 7214 (1987).
- <sup>27</sup>J. M. Delgado, R. K. McMullan, G. Diaz de Delgado, B. J. Wuensch, P. J. Picone, H. P. Jenssen, and D. R. Gabbe, Phys. Rev. B **37**, 9343 (1988).
- <sup>28</sup>B. Dabrowski, D. G. Hinks, J. D. Jorgensen, K. Zhang, and C. U. Segre, Bull. Am. Phys. Soc. **33**, 557 (1988); see also, B. Dabrowski, D. G. Hinks, J. D. Jorgensen, K. Zhang, L. Soderholm, D. R. Richards, and C. U. Segre (unpublished).
- <sup>29</sup>B. Morosin, J. D. Jorgensen, J. E. Schirber, E. L. Venturini, and D. S. Ginley, in *High-Temperature Superconductors II*, edited by D. W. Capone II, W. H. Butler, B. Batlogg, and C. W. Chu, extended abstracts from the Materials Research Society Meeting, Reno, NV, 1988 (Materials Research Society, Pittsburgh, PA, 1988), pp. 259–162.
- <sup>30</sup>G. Aeppli, R. J. Cava, E. J. Ansaldo, J. H. Brewer, S. R. Kreitzman, G. M. Luk, D. R. Noakes, and R. F. Kiefl, Phys. Rev. B **35**, 7129 (1987).
- <sup>31</sup>W. J. Kossler, J. R. Kempton, X. H. Yu, H. E. Schone, Y. J. Uemura, A. R. Moodenbaugh, M. Suenaga, and C. E. Stronach, Phys. Rev. B **35**, 7133 (1987).
- <sup>32</sup>J. D. Jorgensen, J. Faber, Jr., J. M. Carpenter, R. K. Crawford, J. R. Haumann, R. L. Hitterman, R. Kleb, G. E. Ostrowski, F. J. Rotella, and T. G. Worlton, J. Appl. Crystallogr. (to be published).
- <sup>33</sup>J. D. Jorgensen and J. Faber, Jr., Argonne National Laboratory Report No. ANL-82-80, 1983 (unpublished), pp. 105–114.
- <sup>34</sup>R. B. VonDreele, J. D. Jorgensen, and C. G. Windsor, J. Appl. Crystallogr. **15**, 581 (1982).
- <sup>35</sup>J. Zhou, S. Sinha, and J. B. Goodenough, Phys. Rev. B (to be published).